Microelectronic Engineering 144 (2015) 61–67

Contents lists available at ScienceDirect

Microelectronic Engineering

journal homepage: www.elsevier.com/locate/mee

Characterization and bio-binding ability study on size-controllable highly monodisperse magnetic nanoparticles

L. Li [a], A. Ruotolo [b], C.W. Leung [c], C.P. Jiang [a], P.W.T. Pong [a,*]

[a] Department of Electrical and Electronic Engineering, The University of Hong Kong, Hong Kong
[b] Department of Physics and Materials Science, City University of Hong Kong, Hong Kong
[c] Department of Applied Physics, Hong Kong Polytechnic University, Hong Kong

ARTICLE INFO

Article history:
Received 22 October 2014
Received in revised form 24 March 2015
Accepted 30 March 2015
Available online 4 April 2015

Keywords:
Magnetic nanoparticle
Amphiphilic copolymer
Superparamagnetic
Bio-binding ability

ABSTRACT

With the advances in micro-/nano-electronic technology, the development of portable lab-on-chip biodetection device by utilizing magnetic nanoparticles as bio-probes and magnetic field sensor as signal detector has attracted considerable interests in healthcare area. Magnetic probes with required sizes are crucial in quantitative magnetic bio-detection for specific bio-analytes. The objective of this study was to synthesize and characterize amphiphilic co-polymer coated magnetic iron oxide nanoparticles with tunable sizes and study their bio-binding ability. Transmission electron microscopy (TEM), dynamic light scattering (DLS), Fourier transform infrared spectrometer (FT-IR), thermogravimetric analyzer (TGA), and vibrating sample magnetometer (VSM) were employed to investigate the particle dimension, hydrodynamic size, surface property, mass ratio of surface surfactants, and magnetic behavior. The investigation on their biologically binding ability with bovine serum protein was carried out on thin gold film. The results showed iron oxide nanoparticles with controllable sizes were coated by amphiphilic co-polymer successfully and could be completely transferred and well-dispersed in aqueous solutions. The final products with magnetic core sizes ranging from 6 nm to 17 nm showed superparamagnetic behavior, stable hydrodynamic sizes in aqueous suspensions, and binding ability with bio-molecules, making them promising candidates as magnetic tags for the development of bio-detection devices.

1. Introduction

Portable easy-to-use bio-detection devices for healthcare are important for the early diagnosis, disease screening, and preventing epidemics [1,2]. Advanced micro-/nano-fabrication techniques enable many bio-detection systems to realize the development of miniaturized lab-on-chip devices, such as electrochemical method, fluorescent measurement, mass spectrometry, and magnetic biodetection [3–6]. The magnetic biodetection is one of the most promising techniques for early medical diagnosis as well as in molecular biology research area, due to its high sensitivity and rapid quantitative ability [7,8]. Since most biological samples exhibit no magnetic background, this kind of biodetection technology can be performed in visually obscure biological samples without any further processing. In recent years, different magnetic signal detectors, including fluxgates, AC susceptometers, and spintronic sensors have been utilized in many bio-detection studies [9–12]. To improve the bio-sensing sensitivity and accuracy, considerable efforts have been spent on the development of magnetic nanoparticles to understand their behavior and promote their applicability to serve as magnetic bio-probes [8,13].

Magnetic iron oxide nanoparticles (IONPs) are often favored as bio-probes, because they are physiochemical stable, bio-compatible, and environmentally safe [14]. To realize magnetic bio-detection, IONPs must be superparamagnetic with high magnetic moment, monodisperse in aqueous solution, and bear functional groups on their surfaces, such as carboxyl and amino groups, in order to conjugate with biologically active agents. Besides, particle size has been found to play an extremely important role [12]. To acquire ultrahigh bio-detection sensitivity by using spintronic sensors, which is needed for detecting single biomolecules, the size of magnetic probes should be comparable to that of the conjugating biomolecules [15]. For multiplexed sensing based on magnetic susceptibility of IONPs, several types of bioanalytes are targeted by magnetic nanoparticles with different sizes. The maximum imaginary components of their magnetic susceptibility exhibit different frequencies from each other and thus they can be distinguished. This detection mechanism relies on high uniformity of particle size of the IONPs [16]. Therefore, it is worthwhile to find a facile and reliable method

* Corresponding author. Tel.: +852 2857 8491; fax: +852 2559 8738.
E-mail address: ppong@eee.hku.hk (P.W.T. Pong).

http://dx.doi.org/10.1016/j.mee.2015.03.057
0167-9317/

to develop IONPs with controlled sizes as magnetic tags for biosensing application.

Conventionally, IONPs are synthesized via facile co-precipitation. This method can be easily applied for large-scale production and the products can be directly dispersed in water. Scientists have made great efforts to control the particle size ranging from 2 nm to 17 nm through changing the acidity and ionic strength in the reaction system [17,18]. However, the synthesized IONPs through co-precipitation are highly polydisperse. In recent years, thermal decomposition is developed as one of the synthetic routes to produce IONPs with accurate control of size and morphology with narrow size distribution. Through the thermal decomposition of $Fe(acac)_3$ or iron carboxylate salts, high-quality hydrophobic IONPs can be obtained with several controllable particle diameters [19,20]. Nonetheless, the IONPs produced by thermal decomposition method are usually hydrophobic because of the organic surfactants on their surfaces, and cannot be applied in biological usage directly. Therefore, a possible approach is to make these high-quality IONPs hydrophilically stable and surface functionalized with bio-binding ability.

In the current study, we synthesized magnetic nanoparticles with tunable core sizes through thermal decomposition method followed by phase-transfer into aqueous phase using amphiphilic copolymer. This method yielded well-dispersed magnetic nanoparticle colloidal solutions with particle core sizes ranging from 6 nm to 30 nm. Then we characterized the final products and investigated the particle properties after surface coating with amphiphilic polymer. We also studied the binding ability of these particle products to conjugate with biological molecules on gold thin films because gold is commonly used as bio-sensor surface to adsorb proteins [21,22].

2. Experiments

2.1. Materials

Hydrated iron (III) oxide (FeO(OH)),oleic acid (OA), 1-octadecene, poly(maleic anhydride 1-octadecene) (PMAO), and poly(ethylene glycol) methyl ethers (PEG) were purchased from Sigma–Aldrich (USA). All chemicals were used as received.

2.2. Synthesis of amphiphilic copolymer functionalized magnetic IONPs

Our syntheses were based on thermal decomposition method followed by phase transfer and surface functionalization using amphiphilic copolymer. The preparation of oleic-acid-coated iron oxide nanoparticles (OA-IONPs) was carried out in a three-neck flask equipped with condenser, magnetic stirrer, thermocouple, and heating mantle, following Colvin et al.'s thermal decomposition method [20] with slight modification. Due to the fact that the dissolution of starting material was often challenging and the subsequent reaction would fail because of lack of soluble iron in the experiment, the black bulky grained iron precursor FeO(OH) bought from company (Fig. 1a) was grinded into brown fine powders (Fig. 1b) in an agate mortar before use. After the thermal decomposition reaction of 2 mmol FeO(OH) with oleic acid in 5 g 1-ODE, the final products were precipitated by acetone, washed several times with 1:2 mixture of chloroform and acetone, and extracted by magnetic attraction. The supernatant was discarded, and the particles were redispersed in chloroform. The amount of the produced nanoparticles was typically larger than 0.14 g with a high yield above 90%. The molar ratio R of oleic acid to FeO(OH) was varied from 3 to 7 to control the average size of synthesized particles. Amphiphilic copolymer of PMAO-PEG was synthesized by mixing PMAO and low priced hydroxyl group terminated PEG according to Yang et al.'s protocol [23], and the prepared OA-IONPs were phase transferred into aqueous suspension following the procedures reported by Colvin et al. [24]. The PMAO-PEG functionalized oleic-acid-coated IONPs (PP-OA-IONPs) were collected using strong magnet, and the supernatant including excess PMAO-PEG amphiphilic copolymer was discarded. The supernatant was transparent and colorless, indicating all the IONPs were collected with no loss. The final PP-OA-IONPs aqueous solution obtained could pass through a 0.22 μm nylon syringe filter easily, and showed excellent shelf life of over six months. Park et al. [25] have reported the gram-scale synthesis of magnetic IONPs through similar thermal decomposition method, and there was almost no loss of IONPs during the phase-transfer process in our experiment. Thus, it is possible to upscale the volume of this fabrication technique. Further work should be carried out to realize it.

2.3. Characterization of the magnetic nanoparticles

Transmission electron microscopy (TEM) observation on the IONPs was performed by FEI-Tecnai-G2-F20 using carbon-coated copper grids. Particle size distribution data were analyzed by ImageJ. The magnetic properties of nanoparticles were measured using a cryogenic vibrating sample magnetometer (Cryogenic VSM mini-CFM-5T-51-H3). The powder sample was prepared after evaporating the solvent and then wrapped in a Teflon tape. The hysteresis loops were measured at room temperature. The magnetization versus temperature was monitored by zero-field-cooled (ZFC) and field-cooled (FC) curves. ZFC curve was obtained by first cooling the sample down to 10 K under a zero field, then magnetization was measured under an applied filed of 200 Oe while the temperature was increased up to 300 K. FC curve was achieved in the similar way except the sample was cooled down to 10 K under an applied magnetic field of 1 T. Fourier transform infrared (FT-IR) spectra were obtained by a Shimadzu FTIR-8300 spectrometer using KBr pellets. Hydrodynamic size measurement of the IONPs were carried out by dynamic light scattering (DLS) using a Malvern Zetasizer 3000 (Malvern, UK). Iron oxide composition in the final products was determined by using thermal gravimetric analysis (TGA, Perkin-Elmer TGA-7). The mass loss from 5 mg to 10 mg of lyophilized sample was monitored under N_2 at temperatures from 50 °C to 650 °C at a rate of 30 °C/min. The investigation of the binding ability of PP-OA-IONPs with biological molecules was based on the reported procedure [26,27]. In brief, silicon wafers capped with a 200 nm thick gold layer were prepared, and further coated with bovine serum albumin (BSA) through the physical adsorption of protein to the gold surface [22]. After introducing the magnetic nanoparticle sample onto the gold surface, the binding between nanoparticle and BSA could be achieved through the conjugation of carboxyl groups of the nanoparticle to amino groups of the protein via 1-ethyl-3-(3-dimethylaminopropyl) carbodiimide hydrochloride (EDC)/N-hydroxysuccinimide (NHS) coupling chemistry [28,29]. After overnight reaction at 4 °C, the substrate was washed by DI water to remove unbound nanoparticles. An initial investigation on the presence of nanoparticles on the gold surface was carried out using energy dispersive spectroscopy (EDS). The blank gold surface without BSA coating served as control.

3. Results and discussion

To evaluate their size and morphology, the synthesized OA-IONPs were examined under TEM (Fig. 2). Highly monodisperse spherical magnetic iron oxide nanoparticles were achieved in our experiments. Their diameters were tuned by varying the molar

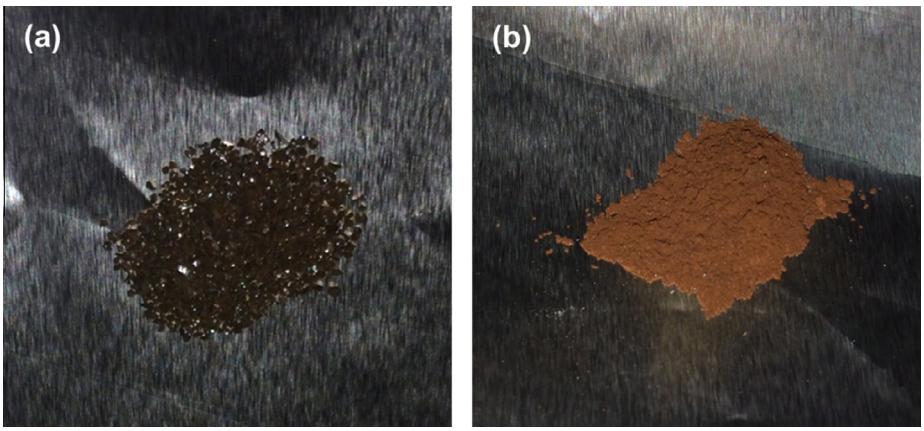

Fig. 1. Iron precursor hydrated iron (III) oxide (FeO(OH)) placed on aluminum foil (a) before and (b) after grinding. The black bulky grained iron precursor was ground into brown fine powder. (For interpretation of the references to color in this figure legend, the reader is referred to the web version of this article.)

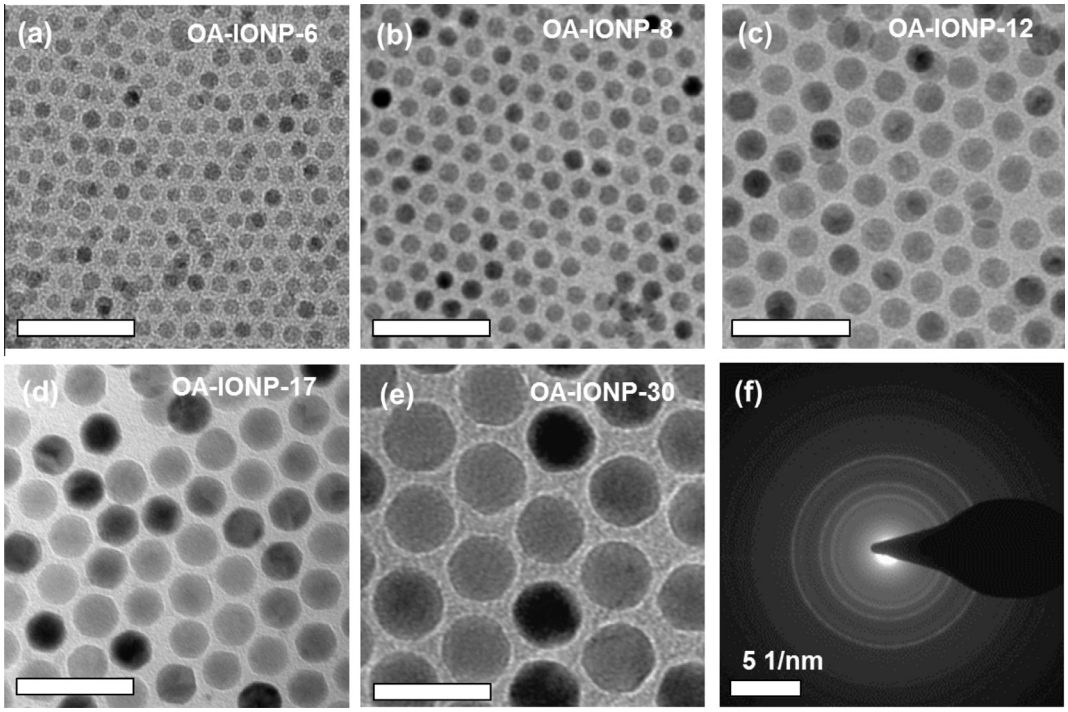

Fig. 2. (a–e) TEM images of oleic-acid-coated magnetic nanoparticles: OA-IONP-6, OA-IONP-8, OA-IONP-12, OA-IONP-17, and OA-IONP-30. Scale bar, 50 nm. (f) SAED pattern of OA-IONP-6.

ratio of ligand/precursor. The initial molar ratio of oleic acid to FeO(OH) in the experiment is denoted as *R*. The average diameters of the OA-IONPs synthesized with varied *R* values are 6.2 ± 1.0 nm (OA-IONP-6, *R* = 3, Fig. 2a), 8.2 ± 0.7 nm (OA-IONP-8, *R* = 4, Fig. 2b), 12.0 ± 0.8 nm (OA-IONP-12, *R* = 5, Fig. 2c), 17.6 ± 1.4 nm (OA-IONP-17, *R* = 6, Fig. 2d), and 30.5 ± 2.3 nm (OA-IONP-30, *R* = 7, Fig. 2e), respectively. The selected area electron diffraction (SAED) pattern of sample OA-IONP-6 (Fig. 2f) shows that the particles are highly crystalline. The difference between magnetite and maghemite is not so obvious because there is very minor difference in electron diffraction of these two phases due to their identical crystal structures [30]. The evolution of average particle size is strongly dependent on the *R* value, and an increase in the oleic acid amount results in the larger particle average size. Similar phenomenon has also been observed by other research groups [20,31]. When ligand concentration is increased in synthesis system, the nucleation step slows down and the particle surface reaction rate is increased. Thus the particle size is mainly controlled by the growth step [32,33]. The more oleic acid is introduced here, the less is the IONP nuclei formed, and their growth tends to form larger particles.

The coercivities of the OA-IONPs samples were obtained from their hysteresis curves measured by VSM at room temperature. OA-IONP-6 (Fig. 3a), OA-IONP-8 (Fig. 3b), OA-IONP-12 (Fig. 3c), and OA-IONP-17 (Fig. 3d) displayed negligible coercivity, thus particle agglomeration can be avoided when there is no applied magnetic field during the biological experimental procedure. As the particle size increased to 30 nm, a clear ferromagnetic behavior was observed for OA-IONP-30 (Fig. 3e) with a coercivity of 120 Oe. Fig. 3f shows the magnified view of the hysteresis loop of OA-IONP-30 as indicated by the red circle in Fig. 3e. The critical diameter for the crossover between superparamagnetic and

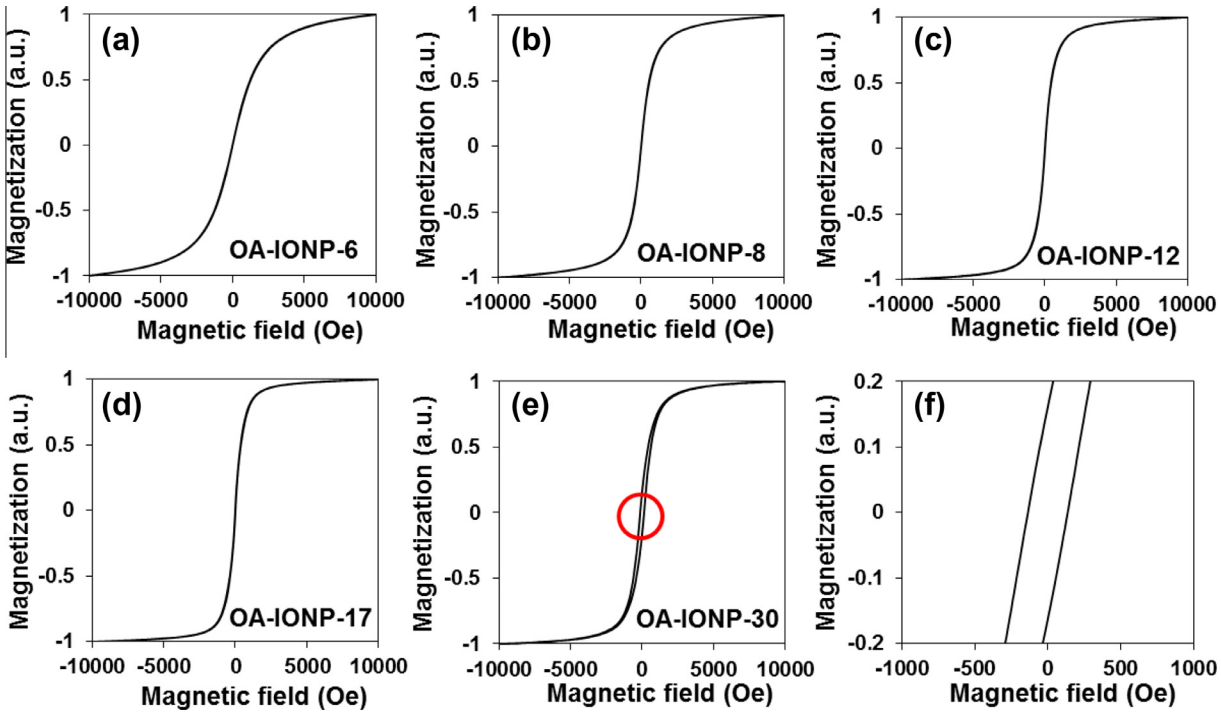

Fig. 3. (a–e) Hysteresis loops of oleic-acid-coated magnetic nanoparticles measured at room temperature: OA-IONP-6, OA-IONP-8, OA-IONP-12, OA-IONP-17, and OA-IONP-30. (f) Magnified view of hysteresis loop of OA-IONP-30 in low magnetic field, as indicated by red circle in (e). (For interpretation of the references to color in this figure legend, the reader is referred to the web version of this article.)

ferromagnetic states at room temperature is reported to be 26.2 nm for magnetite and 34.9 nm for maghemite [34]. The average size of OA-IONP-30 is 30.5 ± 2.3 nm, larger than the critical size for magnetite (26.2 nm) but less than the critical size for maghemite (34.9 nm). The existence of nanoparticles with size beyond the threshold diameter for the superparamagnetic state indicates that the composite of OA-IONP-30 was more like magnetite or a mixture of magnetite and maghemite, rather than pure maghemite. Due to the fact that the ferromagnetic feature might cause particle self-agglomeration when there is no external magnetic field applied, OA-IONP-30 is not favorable to be utilized as magnetic tags in the bio-sensing applications that require switchable magnetism. Thus, only the other four superparamagnetic samples (OA-IONP-6, OA-IONP-8, OA-IONP-12, and OA-IONP-17) were used as magnetic cores in the following phase-transfer experiment.

The formation of PMAO-PEG copolymer and the surface functionalization of OA-IONPs were examined by FT-IR characterization (Fig. 4a). The decrease of 1775 cm^{-1} peak was due to the decomposition of anhydride, and the increase of 1715 cm^{-1} peak indicated the formation of –COOH [24]. The corresponding FT-IR spectrum of the dried PP-OA-IONPs powder shows a characteristic peak of magnetite at 570 cm^{-1} corresponding to Fe–O bending vibration. The peak of 1100 cm^{-1} corresponds to $-CH_2-O-$ in PEG. The peak of 1715 cm^{-1} is attributed to the carboxyl group in PMAO-PEG. In our experiments, all the four kinds of OA-IONPs (OA-IONP-6, OA-IONP-8, OA-IONP-12, and OA-IONP-17) synthesized through thermal decomposition method could be successfully surface modified by PMAO-PEG and completely transferred into water. The photos in Fig. 4b display the phase transfer of OA-IONP-12. With the primary surfactant of oleic acid on the nanoparticle surfaces, OA-IONPs with a hydrophobic nature were dispersed in chloroform (left vial). After surface modified with PMAO-PEG, PP-OA-IONPs were formed and transferred into an aqueous phase (right vial).

The hydrodynamic sizes of PP-OA-IONPs in DI water and in phosphate buffered saline (PBS, pH = 7.4) as measured by DLS are given in Table 1. The average hydrodynamic sizes of PP-OA-IONP-6, PP-OA-IONP-8, PP-OA-IONP-12, and PP-OA-IONP-17 in DI water were 24.9 nm, 26.4 nm, 33.4 nm, and 47.6 nm, respectively, indicating their good dispersion in water. The average hydrodynamic sizes of PP-OA-IONP-6, PP-OA-IONP-8, PP-OA-IONP-12, and PP-OA-IONP-17 in PBS were determined to be 22.8 nm, 25.0 nm, 32.1 nm, and 45.8 nm, respectively. The results demonstrated that PMAO-PEG functionalized nanoparticles retained almost the same hydrodynamic sizes in PBS as in DI water, which ensures their stability during *in vitro* biological experiments using PBS as environment. In the previous study, our group has found that the iron oxide nanoparticles (core size ~ 11 nm) surface functionalized with bilayer of fatty acids showed narrow hydrodynamic sizes of 20–30 nm in DI water, while it showed dramatically increased hydrodynamic sizes of up to 1000 nm in PBS [27]. The results suggest that stronger interaction existed between the PMAO-PEG copolymer and the oleic-acid-coated IONPs, which was less affected by the influence from the salinity and ionic strength in PBS, as compared to the self-assembled bilayer structure of fatty acids around IONP particle surface.

The applicability of nanoparticles as magnetic bio-tags requires a close inspection of their basic magnetic properties. The magnetic property measurement is usually performed through macroscopic magnetometry. However, this method cannot distinguish the magnetic material from the non-magnetic material in the sample. Here, the proportion of magnetic iron oxide cores and non-magnetic surfactant in the sample was obtained through the heating curves of PP-OA-IONP measured by TGA (Fig. 5a). The weight percentage of magnetic iron oxide core in PP-OA-IONP-6, PP-OA-IONP-8, PP-OA-IONP-12, and PP-OA-IONP-17 was determined to be about 40%, 48%, 59%, and 68% respectively. It can be seen that the amount of organic coatings on the particle surfaces in PP-OA-IONP samples decreased as their magnetic core size increased. As the particle core became larger in size, the total surface area providing binding sites for surfactants decreased. Larger nanoparticles have lower surface to volume ratio, so the amount of surfactant on the

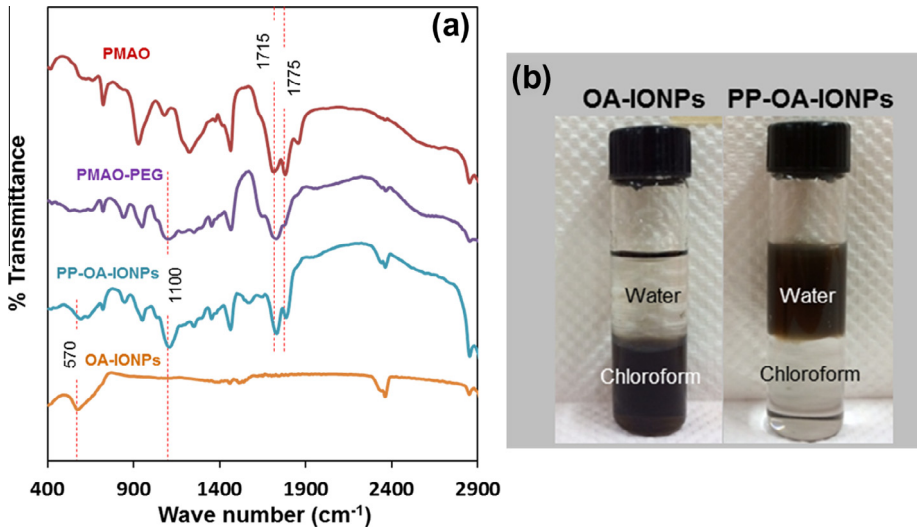

Fig. 4. (a) FT-IR characterization of PMAO, PMAO-PEG copolymer, oleic-acid-coated iron oxide nanoparticles (OA-IONPs), and PMAO-PEG functionalized oleic-acid-coated iron oxide nanoparticles (PP-OA-IONPs). (b) Pictures showing the hydrophobic nature of OA-IONPs, and hydrophilic nature of PP-OA-IONPs.

Table 1
Hydrodynamic size of PMAO-PEG functionalized oleic-acid-coated IONPs (PP-OA-IONPs).

Sample	Mean diameter in DI water (peak analysis by number) (nm)	Mean diameter in PBS (pH = 7.4) (peak analysis by number) (nm)
PP-OA-IONP-6	24.9 ± 13.3	22.8 ± 11.9
PP-OA-IONP-8	26.4 ± 13.5	25.0 ± 12.7
PP-OA-IONP-12	33.4 ± 18.2	32.1 ± 13.3
PP-OA-IONP-17	47.6 ± 24.6	45.8 ± 22.2

particles surface is reduced and the weight percentage of magnetic iron oxide core is higher than the smaller ones [35]. Thus, the TGA results enable important quantitative analysis of the PP-OA-IONP samples with different particle core sizes.

The magnetic hysteresis loops of the PP-OA-IONP samples were obtained from VSM measurement at room temperature (Fig. 5b). All the four PP-OA-IONP samples showed a characteristic superparamagnetic feature with negligible hysteresis at room temperature. By using the TGA results, the saturation magnetization (*Ms*) value weighted by iron oxide cores of PP-OA-IONP-6, PP-OA-IONP-8, PP-OA-IONP-12, and PP-OA-IONP-17 was 50.6 emu/g, 56.7 emu/g, 67.4 emu/g, and 74.8 emu/g, respectively. As the iron oxide core size increased, an increase in Ms value was observed at room temperature, which is consistent with the reported size effect of magnetite or maghemite particle on its saturation magnetization value in the nano regime [31,36]. For the PP-OA-IONP sample with largest iron oxide core size of 17 nm, its Ms value is close to the bulk value (74 emu/g of γ-Fe_2O_3, 90 emu/g for Fe_3O_4). Thus, the PP-OA-IONPs still retained the feature of zero hysteresis and high saturation magnetization value of their iron oxide cores at room temperature after surface functionalized by PMAO-PEG copolymer, which is beneficial for the biosensing application.

The ZFC and FC curves were measured under a magnetic field of 200 Oe in the temperature ranging from 10 K to 300 K, as shown in Fig. 6. For all the samples, the two curves show a divergence point (T_{div}) very close to the maximum point of the ZFC curve (blocking temperature, T_B), suggesting narrow size distribution of the nanoparticles [37]. This is consistent with the observation on the size distribution of iron oxide nanoparticles in the TEM images (Fig. 2a–e). The progressive increase of the FC curve with the decreasing temperature below T_B indicates that the dipolar interaction have been largely reduced due to the surfactants taking the particles apart [38]. The ZFC/FC curves of the four PP-OA-IONP samples displayed a typical magnetic behavior of superparamagnetic nanoparticles, of which the most distinctive feature is the increase of the T_B with the particle size, from ~55 K of the smallest one (PP-OA-IONP-6) to ~225 K of the largest one (PP-

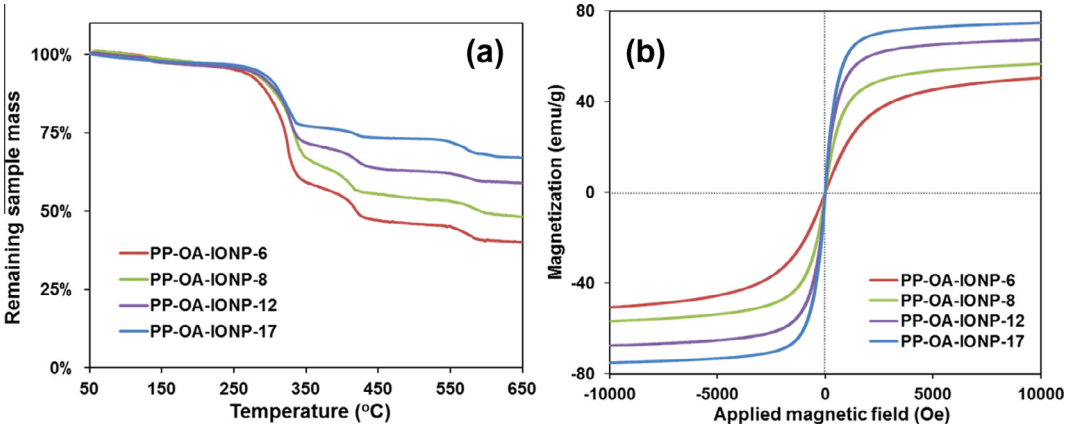

Fig. 5. TGA results and VSM results of amphiphilic co-polymer functionalized oleic-acid-coated iron oxide nanoparticles. (a) Heating curves of PP-OA-IONP-6, PP-OA-IONP-8, PP-OA-IONP-12, and PP-OA-IONP-17. (b) Magnetization curves of PP-OA-IONP-6, PP-OA-IONP-8, PP-OA-IONP-12, and PP-OA-IONP-17 measured at room temperature.

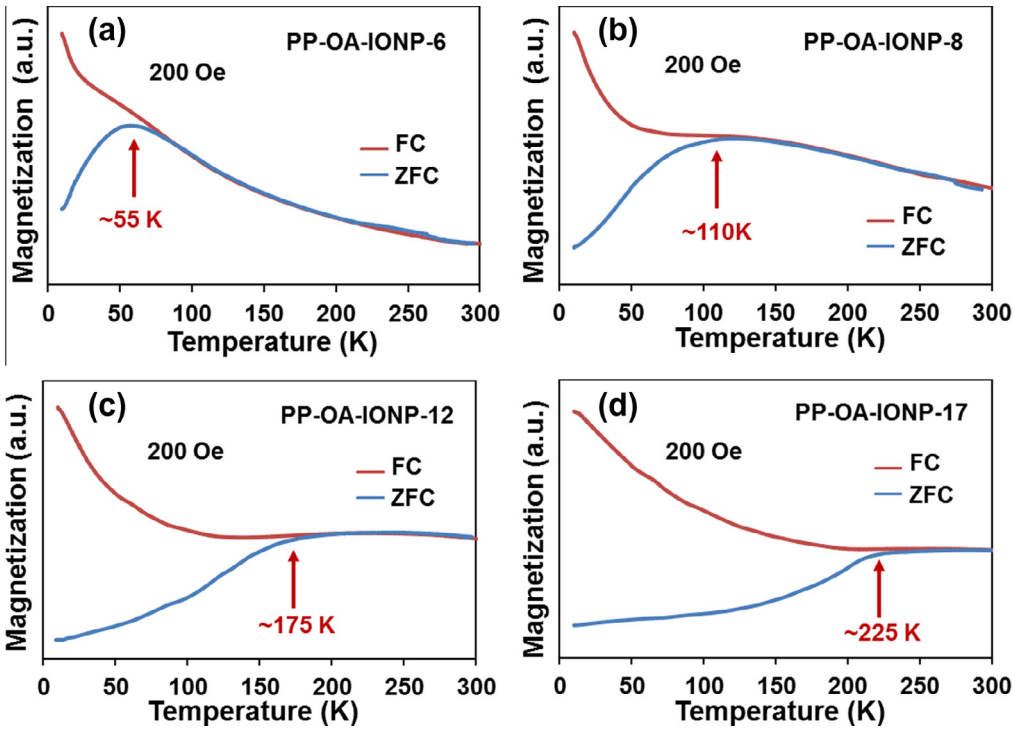

Fig. 6. ZFC/FC curves of the PMAO-PEG amphiphilic co-polymer functionalized oleic-acid-coated iron oxide nanoparticles with different core sizes (a) 6 nm (PP-OA-IONP-6), (b) 8 nm (PP-OA-IONP-8), (c) 12 nm (PP-OA-IONP-12), and (d) 17 nm (PP-OA-IONP-17).

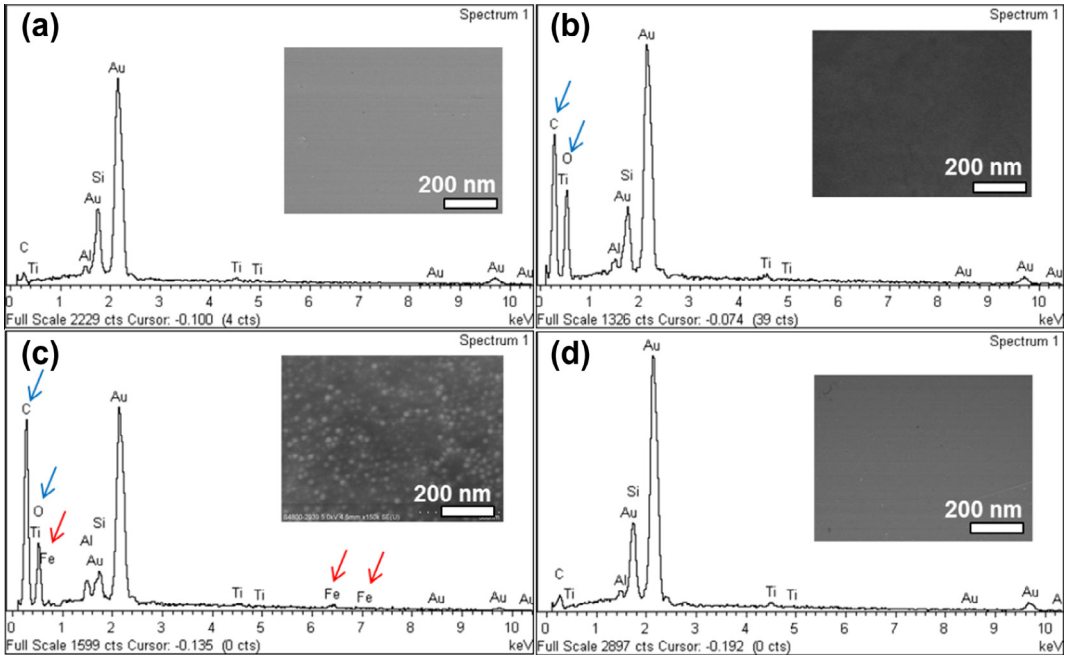

Fig. 7. Elemental EDS analysis of (a) non-BSA pretreated gold surface without treatment of PP-OA-IONP, (b) BSA-pretreated gold surface without treatment of PP-OA-IONP, (c) BSA-pretreated gold surface after the treatment of PP-OA-IONPs, and (d) non-BSA-pretreated gold surface after the treatment of PP-OA-IONP. The presence of carbon and oxygen were indicated by blue arrows in (b) and (c). The presence of iron was indicated by red arrows in (c). Insets show the SEM photos of respective gold surfaces analyzed using EDS. (For interpretation of the references to color in this figure legend, the reader is referred to the web version of this article.)

OA-IONP-17) [39]. One thing to note here is that the surfactant was reported to enhance the particle anisotropy energy, and thus the blocking temperature of naked particles increased after surface modification [40]. In our case, the blocking temperatures of the four samples after functionalized by amphiphilic copolymer were still lower than room temperature. It ensures the superparamagnetic properties of the four PP-OA-IONP products when they are used in bio-sensing application at room temperature.

The experiment to investigate the biologically binding ability of the PMAO-PEG functionalized IONPs samples was carried out with the BSA-pretreated gold surface through a standard EDC/NHS chemical coupling method. Fig. 7 presents the EDS results, and the insets show SEM images of the respective substrates that were analyzed. The PP-OA-IONP-12 sample was used here as a representative example. The elements of Si, Au, Ti, Al, and C come from the non-BSA pretreated silicon substrate capped with gold surface

(Fig. 7a). The presence of oxygen and dramatically increased amount of carbon in Fig. 7b verified the protein coating on the gold surface after pretreated by BSA. After introducing nanoparticles onto the BSA-pretreated gold surface and EDC/NHS coupling procedure, the nanoparticles without protein binding ability were removed during the following washing step by DI water [27]. In Fig. 7c, the principal elements of the BSA-IONP complexes were confirmed by the presence of iron, carbon, and oxygen in the EDS result. The binding of PP-OA-IONPs onto the BSA-pretreated gold surface should be through the free –COOH groups on the outmost layer of the nanoparticles to the $-NH_2$ groups of the BSA via EDC/NHS coupling. Besides, there was no presence of Fe element in the control experiments using non-BSA-pretreated gold surfaces (Fig. 7d). Thus, the initial bio-binding ability study confirms biomolecules binding ability of the PP-OA-IONP samples. They can be potentially applied as magnetic tags for bio-molecules labeling.

4. Conclusion

Here, size-controllable amphiphilic copolymer functionalized oleic-acid-coated iron oxide nanoparticles (PP-OA-IONP) were synthesized. The relevant properties of the products in order to be used as magnetic bio-tags were characterized and discussed. The core sizes of the iron oxide nanoparticles could be tuned by simply varying the initial ratio of starting materials. The polymer coating of particle surface was proven by FT-IR measurement and TGA measurement. The hydrodynamic size of the synthesized nanoparticles in DI water and PBS were determined. The magnetic properties of particles were studied by using VSM. We also investigated the binding ability of these PP-OA-IONPs with BSA through standard procedure on gold thin film. The presence of free carboxyl groups on the outmost layer of the particles provides an avenue for the coupling reactions with proteins and other molecules. For the superparamagnetic iron oxide nanoparticles (6 nm, 8 nm, 12 nm, and 17 nm), our research results demonstrated that the successful coating of amphiphilic co-polymer ensured their good dispersity in aqueous environment, enabled their bio-binding ability with protein, and retained their superparamagnetic property and high saturation magnetization value at room temperature. With tunable core size from 6 nm to 17 nm (tunable hydrodynamic size from ~24 nm to ~47 nm in aqueous solution), these superparamagnetic PP-OA-IONP products have great potential to be applied in the micro-/nano-electronic biomedical engineering. For example, in recent years, the spintronic sensors have been widely utilized as signal detectors in the lab-on-chip bio-detection platforms for point-of-care applications because of their compatibility with the standard CMOS fabrication technology. In this kind of platform, magnetic iron oxide nanoparticles usually serve as biotags, of which the magnetic signal induces the resistance change in spintronic sensor. The resistance variation of spintronic sensor is measured through micro circuit, and the number of magnetic nanoparticles and the amount to targeting bioanalytes are obtained after data analysis [41–43]. To avoid steric hindrance effect and to improve the accuracy of signal analysis, the size of magnetic particle labels should be comparable to that of bioanalytes [44]. Thus, the size-tunable PP-OA-IONPs are highly promising to be applied for the detection of bioanalytes with varied sizes in lab-on-chip biosensors.

Acknowledgments

This work was supported by the Seed Funding Program for Basic Research and Small Project Funding from the University of Hong Kong (201309176231), the RGC-GRF Grant (HKU 704911P), ITF Tier 3 Funding (ITS/104/13), and University Grants Committee of Hong Kong (Contract No. AoE/P-04/08). Assistance from Mr. Frankie Chan (EMU, The University of Hong Kong), Mr. Eric K.S. Cheung (EEE, The University of Hong Kong) and Mr. Dickey Ma (EEE, The University of Hong Kong) is gratefully acknowledged.

References

[1] P. Tallury, A. Malhotra, L.M. Byrne, S. Santra, Adv. Drug Deliv. Rev. 62 (2010) 424–437.
[2] A.E. Cetin, A.F. Coskun, B.C. Galarreta, M. Huang, D. Herman, A. Ozcan, H. Altug, Light Sci. Appl. 3 (2014) e122.
[3] L. Nyholm, Analyst 130 (2005) 599–605.
[4] L. Novak, P. Neuzil, J. Pipper, Y. Zhang, S. Lee, Lab Chip 7 (2007) 27–29.
[5] J. Carlier, S. Arscott, V. Thomy, J. Fourrier, F. Caron, J. Camart, C. Druon, P. Tabourier, J. Micromech. Microeng. 14 (2004) 619.
[6] J. Do, C.H. Ahn, Lab Chip 8 (2008) 542–549.
[7] N. Sanvicens, C. Pastells, N. Pascual, M. Marco, TrAC, Trends Anal. Chem. 28 (2009) 1243–1252.
[8] X. Sun, D. Ho, L.-M. Lacroix, J.Q. Xiao, S. Sun, IEEE Trans. NanoBiosci. 11 (2012) 46–53.
[9] A.K. Bhuiya, M. Asai, H. Watanabe, T. Hirata, Y. Higuchi, T. Yoshida, K. Enpuku, IEEE Trans. Magn. 48 (2012) 2838–2841.
[10] K. Park, T. Harrah, E.B. Goldberg, R.P. Guertin, S. Sonkusale, Nanotechnology 22 (2011) 085501.
[11] W. Shen, B.D. Schrag, M.J. Carter, J. Xie, C. Xu, S. Sun, G. Xiao, J. Appl. Phys. 103 (2008). 07A306-307A306-303.
[12] L. Li, C. Leung, P. Pong, J. Nanoelectron. Optoelectron. 8 (2013) 397–414.
[13] W. Wang, Y. Wang, L. Tu, Y. Feng, T. Klein, J.-P. Wang, Sci. Rep. 4 (2014).
[14] S.I. Park, J.H. Lim, J.H. Kim, H.I. Yun, C.O. Kim, J. Magn. Magn. Mater. 304 (2006) e406–e408.
[15] G. Li, S. Sun, R.J. Wilson, R.L. White, N. Pourmand, S.X. Wang, Sens. Actuators A 126 (2006) 98–106.
[16] M. Strömberg, T. Zardán, Anal. Chem. 81 (2009) 3398–3406.
[17] J.-P. Jolivet, É. Tronc, C. Chanéac, C. R. Chim. 5 (2002) 659–664.
[18] B. Sahoo, S.K. Sahu, P. Pramanik, J. Mol. Catal. B Enzym. 69 (2011) 95–102.
[19] S. Sun, H. Zeng, J. Am. Chem. Soc. 124 (2002) 8204–8205.
[20] W.Y. William, J.C. Falkner, C.T. Yavuz, V.L. Colvin, Chem. Commun. (2004) 2306–2307.
[21] R.L. Edelstein, C.R. Tamanaha, P.E. Sheehan, M.M. Miller, D.R. Baselt, L.J. Whitman, R.J. Colton, Biosens. Bioelectron. 14 (2000) 805–813.
[22] C.S.S.R. Kumar, Nanocomposites, John Wiley & Sons, 2010.
[23] Y. Ning, H. Zhang, J. Han, C. Yang, Y. Liu, D. Zhou, B. Yang, J. Mater. Chem. 21 (2011) 6837–6843.
[24] W.Y. William, E. Chang, C.M. Sayes, R. Drezek, V.L. Colvin, Nanotechnology 17 (2006) 4483.
[25] J. Park, K. An, Y. Hwang, J.-G. Park, H.-J. Noh, J.-Y. Kim, J.-H. Park, N.-M. Hwang, T. Hyeon, Nat. Mater. 3 (2004) 891–895.
[26] B.G. Nidumolu, M.C. Urbina, J. Hormes, C.S.S.R. Kumar, W.T. Monroe, Biotechnol. Prog. 22 (2006) 91–95.
[27] L. Li, K. Mak, C. Leung, K. Chan, W. Chan, W. Zhong, P. Pong, IEEE Trans. Magn. 48 (2012) 3299–3302.
[28] K.D. Wittrup, G.L. Verdine, Protein Engineering for Therapeutics, Elsevier Sci. Technol. (2012).
[29] G.T. Hermanson, Bioconjugate Techniques, Academic Press, 2013.
[30] J. Tang, M. Myers, K.A. Bosnick, L.E. Brus, J. Phys. Chem. B 107 (2003) 7501–7506.
[31] A. Demortiere, P. Panissod, B. Pichon, G. Pourroy, D. Guillon, B. Donnio, S. Begin-Colin, Nanoscale 3 (2011) 225–232.
[32] L.M. Bronstein, X. Huang, J. Retrum, A. Schmucker, M. Pink, B.D. Stein, B. Dragnea, Chem. Mater. 19 (2007) 3624–3632.
[33] J. van Embden, J.E. Sader, M. Davidson, P. Mulvaney, J. Phys. Chem. C 113 (2009) 16342–16355.
[34] K.D. Sattler, Handbook of Nanophysics: Nanoparticles and Quantum Dots, CRC Press, 2010.
[35] J.K. Bailey, C.J. Brinker, M.L. Mecartney, J. Colloid Interface Sci. 157 (1993) 1–13.
[36] M. Mahdavi, M.B. Ahmad, M.J. Haron, F. Namvar, B. Nadi, M.Z.A. Rahman, J. Amin, Molecules 18 (2013) 7533–7548.
[37] D. Predoi, V. Kuncser, E. Tronc, M. Nogues, U. Russo, G. Principi, G. Filoti, J. Phys. Condens. Matter 15 (2003) 1797.
[38] P. Guardia, B. Batlle-Brugal, A. Roca, O. Iglesias, M. Morales, C. Serna, A. Labarta, X. Batlle, J. Magn. Magn. Mater. 316 (2007) e756–e759.
[39] I. Castellanos-Rubio, M. Insausti, E. Garaio, I. Gil de Muro, F. Plazaola, T. Rojo, L. Lezama, Nanoscale 6 (2014) 7542–7552.
[40] M. Mazur, A. Barras, V. Kuncser, A. Galatanu, V. Zaitzev, K.V. Turcheniuk, P. Woisel, J. Lyskawa, W. Laure, A. Siriwardena, Nanoscale 5 (2013) 2692–2702.
[41] R.S. Gaster, D.A. Hall, S.X. Wang, Lab Chip 11 (2011) 950–956.
[42] S.G. Grancharov, H. Zeng, S. Sun, S.X. Wang, S. O'Brien, C. Murray, J. Kirtley, G. Held, J. Phys. Chem. B 109 (2005) 13030–13035.
[43] R.L. Millen, T. Kawaguchi, M.C. Granger, M.D. Porter, M. Tondra, Anal. Chem. 77 (2005) 6581–6587.
[44] R.S. Gaster, D.A. Hall, C.H. Nielsen, S.J. Osterfeld, H. Yu, K.E. Mach, R.J. Wilson, B. Murmann, J.C. Liao, S.S. Gambhir, Nat. Med. 15 (2009) 1327–1332.